Chemical and Process Engineering 2011, 32 (1), 33-40
DOI: 10.2478/v10176-011-0003-9

LOCAL DISTRIBUTIONS OF FLUID VELOCITY AND TRACER CONCENTRATION IN A TANK REACTOR

Łukasz Makowski*, Wojciech Orciuch

Warsaw University of Technology, Faculty of Chemical and Process Engineering,
ul. Waryńskiego 1, 00-645 Warsaw, Poland

The aim of the project was to collect experimental data regarding local distributions of fluid velocity and inert tracer concentration in a tank reactor with turbulent flow. The experiments were performed in a microscale in a region of tracer fluid injection. The results of experiments can be used for direct validation of currently developed CFD models, particularly for time-dependent mixing models used in LES.

Keywords: tracer concentration, fluid velocity, PIV, PLIF, LES

1. INTRODUCTION

Stirred chemical tank rectors are widely represented in industrial processes. Understanding complex flow dynamics is crucial to the explanation of many processes that occur in reactors (Lee and Yianneskis,1998; Wu and Patterson, 1989; Bałdyga and Makowski, 2004). These complex, often turbulent, flowfields may be predicted through numerical solutions of Navier-Stokes equations. To account for the full nonlinear multi-scale effects of turbulence, the N-S equations must be solved resolving the micro-scale effects, which is not possible for almost all technically important flows. A full simulation of turbulent flows resolving all scales involved, the so-called direct numerical simulation (DNS), is restricted to simplest geometry and low Reynolds numbers (Bałdyga and Bourne, 1999; Jaworski, 2005). The second way is to use statistical averaging models, Reynolds-averaged Navier-Stokes equations (RANS). These models are closed by empirical equations for extra unknown quantities, such as turbulent kinetic energy and its dissipation rate. RANS models offer a cheap and simple way to approximate coarse scale behavior of turbulent flows, but they give only rough approximations of local instantaneous flows. In many cases there are critical important quantities of the flow, like the Reynolds stresses, which are approximated poorly by RANS models. A solution of this problem is modeling of turbulence using large eddy simulation (LES). The idea is to resolve large scales which can be represented by a computational grid and to model structures smaller than the resolution of the grid by subgrid-scale models. Although LES needs finer grids than RANS simulations, LES gives much better accuracy for important turbulence quantities and thus by using LES one gets more information about processes important from a technical point of view.

The aim of this work was to collect experimental data regarding local microstructures of fluid flow and inert tracer concentration in a tank reactor with turbulent flow. The results of experiments, performed with resolution of the level of several microns, can be used for direct validation of currently developed CFD models, particularly for time-dependent mixing models used in large eddy simulations. The main problem in modeling fast processes in turbulent flow is correct description of mixing mechanisms in

*Corresponding author, e-mail: l.makowski@ichip.pw.edu.pl

closest surroundings of a feeding point. Therefore investigations of velocity and concentration distribution in this area were important in our work. Experimental results were compared with predictions of the *k-ε* model and results from LES modeling of scalar mixing.

2. EXPERIMENTAL SYSTEM

Experiments were performed in a flat-bottom tank reactor of diameter $T = 0.28$ m and height equal to T. The reactor was equipped with four blades of width equal to $T/8$ and a Rushton turbine of diameter $D = 0.08$ m. The turbine disc was placed at the distance of $T/3$ from the bottom. Two vertical feeding pipes were introduced inside from the top of the tank. Injection pipe for tracer solution (o.d. 1.8×10^{-3} m, i.d. 1.3×10^{-3} m) was placed 0.075 m from the tank axis. Outlet of this pipe was located on the level of the turbine disc. Second feeding pipe (o.d. 8.0×10^{-3} m, i.d. 5.0×10^{-3} m) was located on the opposite side of the turbine. The tank was operated in a continuous mode and the second feeding pipe was used to supply tank with water and keep constant value of mean tracer concentration in the tank. Stirrer rotation speed N changed from 3.33 to 5.0 s^{-1}. Two values of tracer solution injection flow rate q were tested: 1.33×10^{-6} and 2.00×10^{6} m^3 s^{-1}. The outlet from the tank was located in the tank cover. Water containing seeding particles and dissolved fluorescent tracer was fed through the tracer injection pipe. Water with the particles was pumped through the second injection pipe. Cylindrical wall of the tank was surrounded by rectangular water jacket. All vertical walls of the system were made of glass. The experiments were performed at a constant temperature equal to 22°C. All the details of the reactor's geometry are shown in Figure 1.

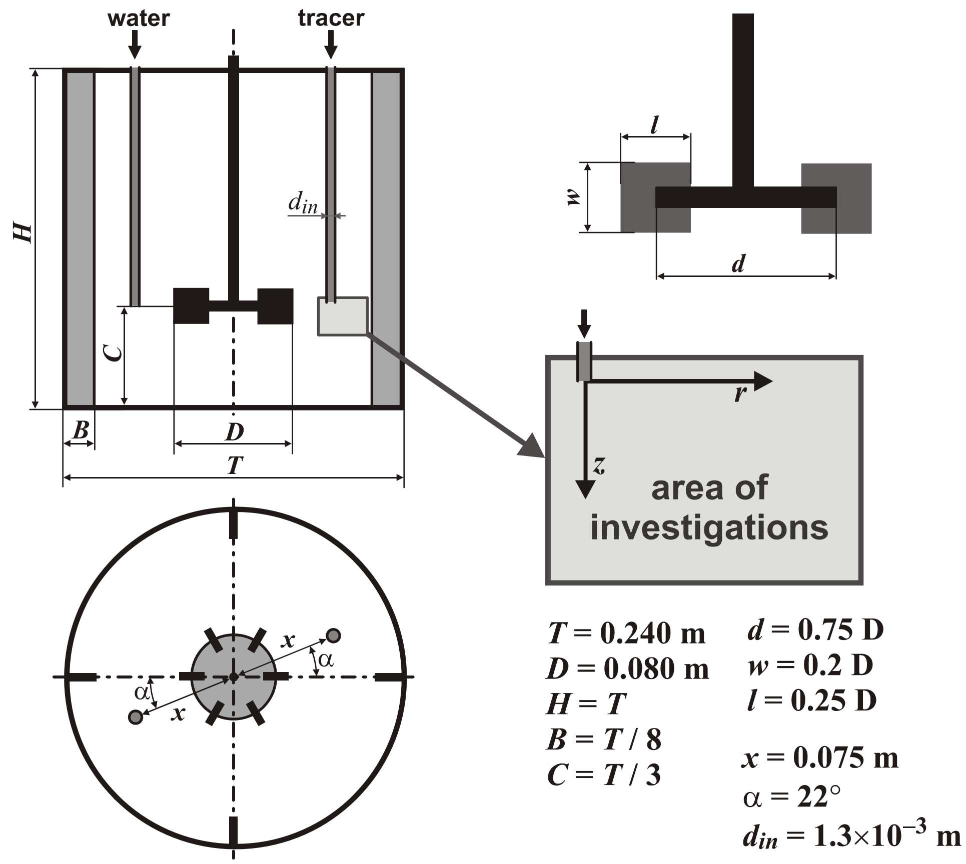

Fig. 1. Schematic presentation of the stirred tank reactor, investigation area and coordination system

3. HYDRODYNAMICS AND MIXING

3.1. Measurements

Local, instantaneous values of fluid velocity and passive tracer concentration were measured simultaneously using two techniques: particle image velocimetry (PIV) and planar laser induced fluorescence (PLIF). Double-cavity Nd-YAG laser 532 nm with energy equal to 50 mJ per pulse was used. Laser beam was transformed to a collimated planar laser sheet of thickness $\delta \approx 300$ µm. The laser sheet crossed the experimental system vertically through the axis of the tracer injection pipe and the axis of the tank. The investigation area was located directly below the outlet of the pipe (Fig. 1). Polyamide spherical particles of average size equal to 20 µm were used as seeding particles for PIV measurements. The particles were equally dispersed in the inlet solutions and the inside of the tank. Rhodamine B was used as the fluorescent tracer for PLIF measurements and its concentration in the inlet solution was equal to 0.2 g m^{-3}. Spatial resolution of PLIF measurements results from resolution of digital images and thickness of the laser sheet (Mortensen et al., 2004); in our case it was 18×18×300 µm. Spatial resolution of PIV measurements also depends on the size of a sampling window and in this work it was 264×264×300 µm.

3.1. Numerical simulations

Simulations of hydrodynamics were performed using the CFD code Ansys FLUENT, using standard *k-ε* and LES models. The numerical grid consisted of 3 301 216 hexahedral computational cells. Convergence of computations was regarded as satisfactory when the total normalized residuals were smaller than 10^{-6}. Effects of the small scale in LES were modeled using a dynamic sub-grid-scale (SGS) model. The sub-grid-scale scalar flux was calculated using a gradient-diffusion model with turbulent diffusion obtained as a quotient of a SGS turbulent kinematic viscosity (resulting from the dynamic SGS model) and a SGS turbulent Schmidt number equal to 0.4 ($Sc_{SGS} = \nu_{SGS}/D_{SGS}$) (Jaworski, 2005; Fox, 2003). Mixture fraction f was also predicted in the *k-ε* and LES modeling with $f = 1$ in the tracer solution injection pipe and $f = 0$ in the second feeding pipe.

The *k-ε* model was completed with the multiple-time-scale turbulent mixer model (TMM) (Bałdyga, 1989) to predict distributions of the mixture fraction variance σ_s^2 . TMM enables prediction of the distribution of the concentration variance, as well as its inertial-convective, viscous-convective and viscous-diffusive components. The distributions of the concentration variance components, σ_i^2, are modeled using the gradient diffusion approximation:

$$\frac{\partial \sigma_i^2}{\partial t} + \langle u_j \rangle \frac{\partial \sigma_i^2}{\partial x_j} = \frac{\partial}{\partial x_j}\left[\left(D_m + D_T \right) \frac{\partial \sigma_i^2}{\partial x_j} \right] + R_{Pi} - R_{Di} \quad \text{for } i = 1,2,3 \tag{1}$$

where R_{Pi} and R_{Di} represent the production and dissipation terms:

- σ_1^2 is produced from gradients of $\langle f \rangle$:

$$R_{P1} = -2\langle u_j' f' \rangle \frac{\partial \langle f \rangle}{\partial x_j} = 2D_T \left(\frac{\partial \langle f \rangle}{\partial x_j} \right)^2 \tag{2}$$

and is dissipated due to the inertial-convective reduction of the scale of inhomogeneity, producing σ_2^2.

$$R_{D1} = R_{P2} = \frac{\sigma_1^2}{\tau_S} \text{ with } \tau_S = \frac{1}{R}\frac{k}{\varepsilon} \tag{3}$$

- σ_2^2 decays due to viscous-convective shrinking of component slabs, producing σ_3^2

$$R_{D2} = R_{P3} = E\sigma_2^2 \text{ with } E = 0.058\left(\frac{\varepsilon}{\nu}\right)^{1/2} \tag{4}$$

- σ_3^2 is dissipated due to molecular diffusion in deforming, shrinking slabs

$$R_{D3} = G\sigma_3^2 \text{ with } G = E\left(0.303 + \frac{17050}{Sc}\right) \tag{5}$$

4. RESULTS AND DISCUSSION

For each experiment, PIV and PLIF results consisted of 2000 two-dimensional maps containing distributions of local velocity vectors and distributions of tracer concentration. Each map represented instantaneous situation observed during turbulent mixing. The PIV measurements gave two components of velocity vectors – radial and axial. Therefore, a value of velocity (length of velocity vector) was calculated using these two components only. The collected results from PLIF measurements allowed, after statistical procedure, to define the mixture fraction for two mixed fluids:

$$f = \frac{\textit{volume of tracer solution}}{\textit{volume of mixture}} = \frac{\textit{tracer concentration in a mixture}}{\textit{tracer concentration at the inlet}} \tag{6}$$

Results are presented using radial and axial directions (r and z), as shown in Fig. 1, with a centre of coordinate system located in the centre of the outlet of the tracer solution injection pipe. Figure 2 shows the measured and predicted distributions of mean velocity values $\langle u \rangle$ and mean mixture fraction $\langle f \rangle$ for $q = 1.33\times10^{-6}$ m^3 s^{-1} and $N = 5.0$ s^{-1}, whereas Figure 3 shows examples of instantaneous distributions for the same process conditions. Figure 4 presents radial distributions of mean mixture fraction for two different distances from the outlet of the injection pipe. One can see that the results of the LES modeling better agree with experiments than the results of the k-ε model, particularly in the area directly below the injection. However, in LES modeling, the mixing zone is too large, which shows the need to improve the sub-grid model for scalar flux. It is a well known problem with SGS turbulent Schmidt number approach when the velocity field if fully resolved (the Navier-Stokes equations are solved directly), yielding $\nu_{SGS} = 0 \Rightarrow D_{SGS} = 0$, while some subgrid scalar fluctuations still exist.

It was observed that the difference between the k-ε model predictions and the measured data increased with an increase of injection velocity and with a decrease of stirrer rotation speed for both flow and concentration. Figures 5 and 6 present distributions of the variance of the mixture fraction for $q = 2.00\times10^{-6}$ m^3 s^{-1} and $N = 3.33$ s^{-1}. Spatial resolution of the PLIF measurements was not enough to recognize concentration variance in the smallest scales. Therefore, the experimentally determined variance is smaller than the one predicted by TMM.

It was observed and experimentally proved (Bałdyga et al., 2001) that for small mean residence times the k-ε model underrate the final selectivity of chemical reaction, which was probably the result of underrating the range of the mixing zone (and probably the chemical reaction zone). The results presented in this work confirmed this supposition.

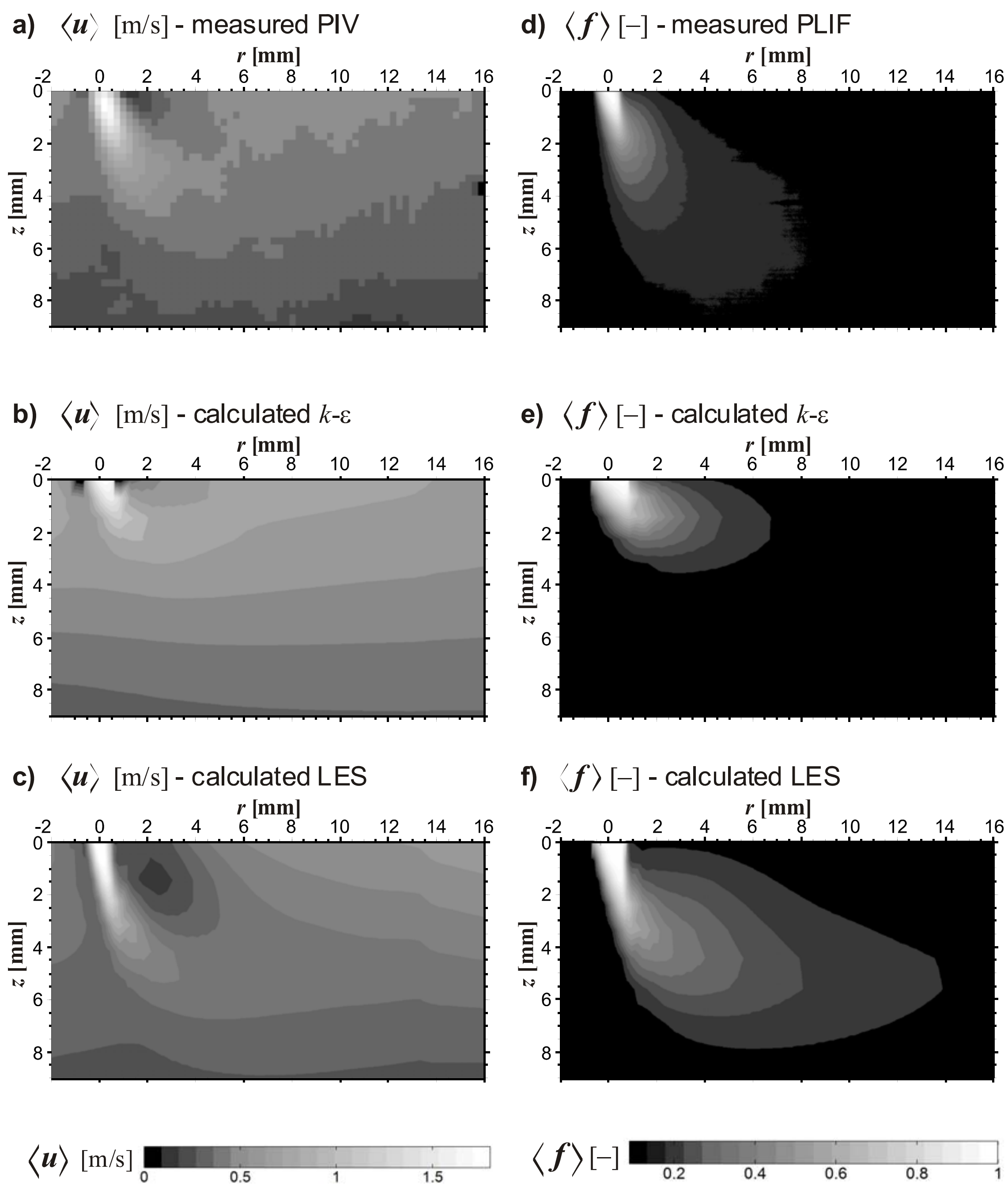

Fig. 2. Distributions of mean velocity value $\langle u \rangle$ and mean mixture fraction $\langle f \rangle$ for $q = 1.33\times10^{-6}$ m^3 s^{-1} and N =5.0 s^{-1} a) $\langle u \rangle$ measured by PIV, b) $\langle u \rangle$ calculated with k-ε model, c) $\langle u \rangle$ calculated with LES, d) $\langle f \rangle$ measured by PIV, e) $\langle f \rangle$ calculated with k-ε model, f) $\langle f \rangle$ calculated with LES

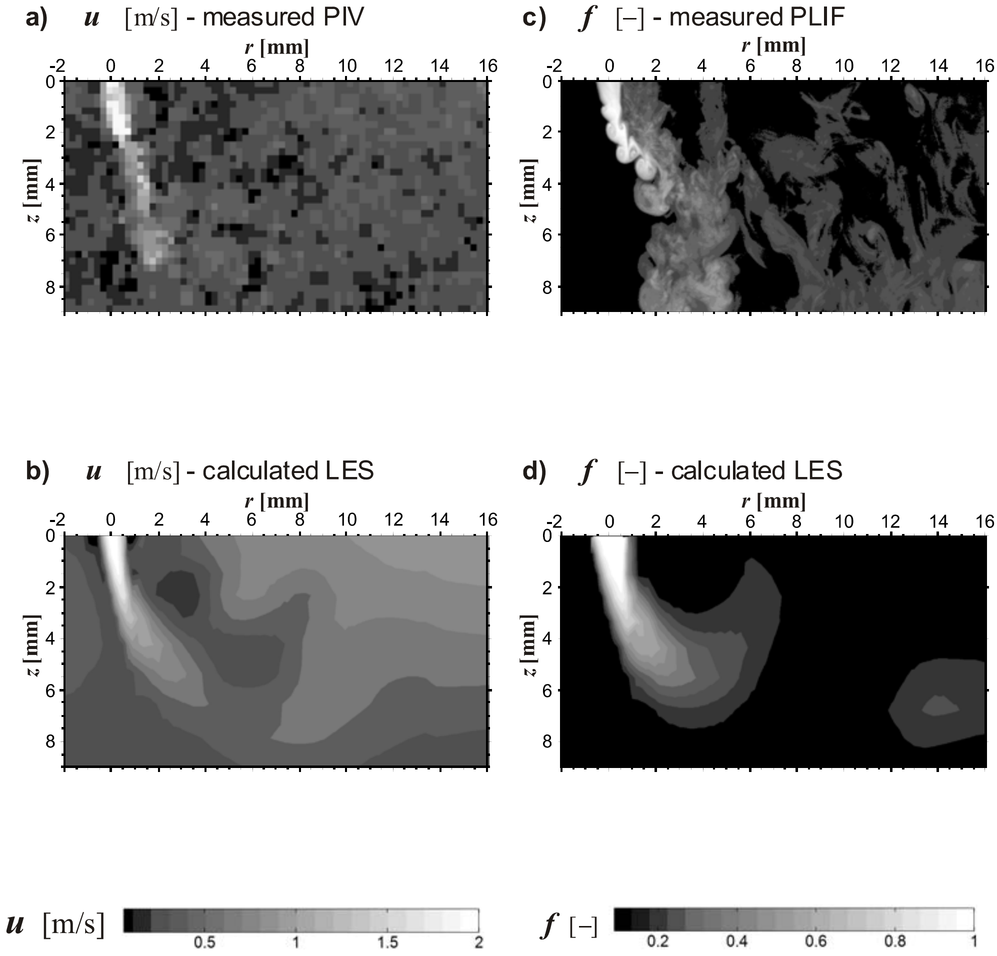

Fig. 3. Examples of instantaneous distributions of velocity value u and mixture fraction f, $q = 1.33\times10^{-6}$ m^3 s^{-1} and $N = 5.0$ s^{-1}; a) u measured by PIV, b) u calculated with LES, c) f measured by PLIF, d) f calculated with LES

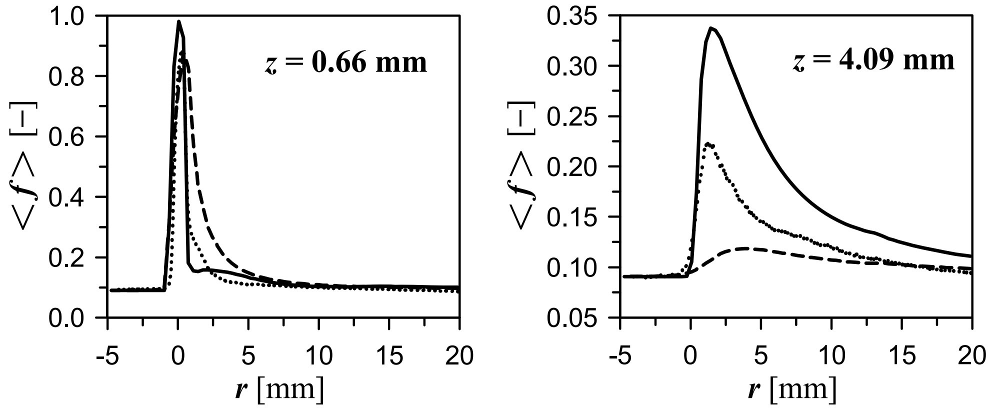

Fig. 4. Radial distributions of mean mixture fraction $\langle f \rangle$ for $q = 1.33\times10^{-6}$ m^3 s^{-1} and $N = 5.0$ s^{-1} for two different distances from the injection point (z = 0.66 mm, z = 4.09 mm), points – measured by PLIF, solid lines – calculated with LES, dashed lines – calculated with k-ε model

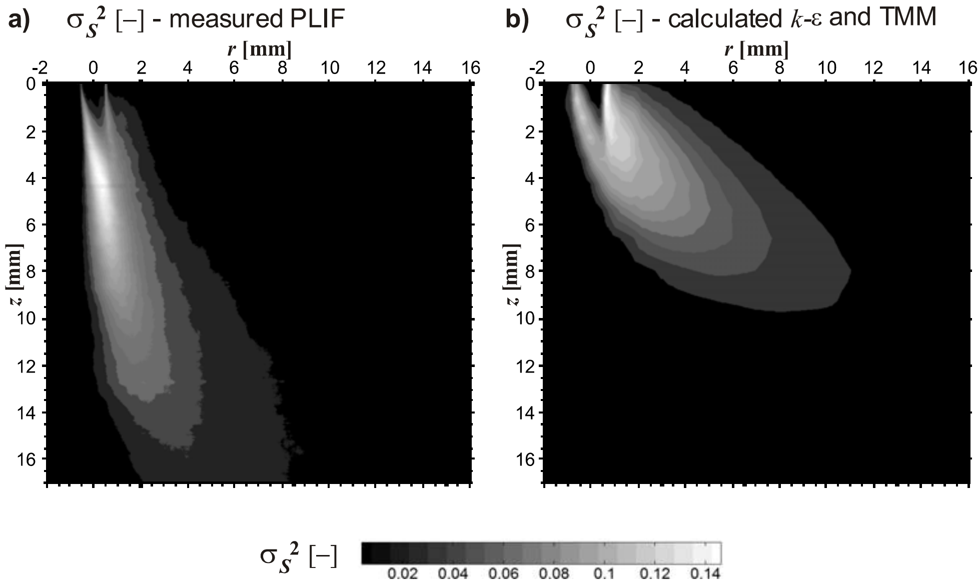

Fig. 5. Distributions of mixture fraction variance σ_s^2 for $q = 2.00\times10^{-6}$ m^3 s^{-1} and $N = 3.33$ s^{-1}; a) σ_s^2 measured by PLIF, b) σ_s^2 calculated with k-ε model and the TMM

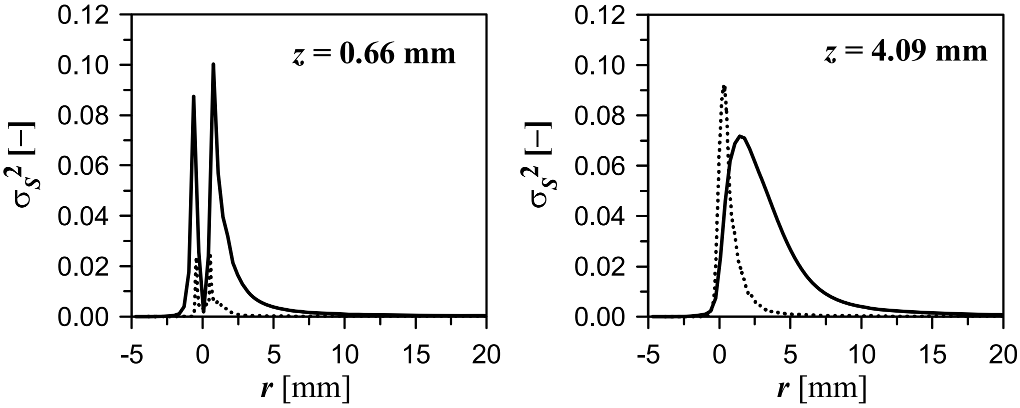

Fig. 6. Radial distributions of mixture fraction variance σ_s^2 for $q = 2.00\times10^{-6}$ m^3 s^{-1} and $N = 3.33$ s^{-1}, points - measured by PLIF, lines – calculated with k-ε model and the TMM

5. CONCLUSIONS

In this study LES and *k-ε* models are used to predict turbulent flow and mixing in the tank reactor with Ruston turbine. The predicted results are compared with experiments obtained by PIV and PLIF techniques. Time-averaged LES results of velocity distributions are in good agreement with the experimental results. The size of the mixing zone of mean mixture fraction is larger than that observed in the experiments; this problem can be probably solved by developing a subgrid scale model for turbulent diffusivity.

A comparison of mixture fraction variance obtained from the numerical calculations (*k-ε* model) and PLIF experiments gives a similar shape of spatial distributions but differs in values. The problem lays in insufficient spatial resolution of the PLIF measurements.

SYMBOLS

D_m	molecular diffusion coefficient, $m^2\ s^{-1}$
D_{SGS}	SGS turbulent diffusion coefficient, $m^2\ s^{-1}$
D_T	turbulent diffusion coefficient, $m^2\ s^{-1}$
E	engulfment parameter, s^{-1}
f	mixture fraction, -
G	molecular diffusion parameter, s^{-1}
k	kinetic energy of turbulence, $m^2\ s^{-2}$
N	stirrer rotation speed, s^{-1}
q	injection flow rate, $m^3\ s^{-1}$
Sc	Schmidt number, -
Sc_{SGS}	SGS turbulent Schmidt number, -
u	velocity, $m\ s^{-1}$
ε	rate of energy dissipation, $m^2\ s^{-3}$
ν	kinematic viscosity, $m^2\ s^{-1}$
ν_{SGS}	SGS turbulent kinematic viscosity, $m^2\ s^{-1}$
σ_S^2	mixture fraction variance, -
τ_S	time scale for the inertial-convective mixing, s
$\langle\ \rangle$	time average value

REFERENCES

Bałdyga J., 1989. Turbulent mixer model with application to homogeneous, instantaneous chemical reactions. *Chem. Eng. Sci.*, 44, 1175-1182. DOI:10.1016/0009-2509(89)87016-2.

Bałdyga J., Bourne J. R., 1999. *Turbulent Mixing and Chemical Reactions*, Wiley, Chichester.

Bałdyga J., Henczka M., Makowski Ł., 2001. Effects of Mixing on Parallel Chemical Reactions in a Continuous-Flow Stirred-Tank Reactor. *Chem. Eng. Res. Des.*, 79, 895-900. DOI:10.1205/02638760152721109.

Bałdyga J., Makowski Ł., 2004. CFD Modelling of Mixing Effects on the Course of Parallel Chemical Reactions Carried out in a Stirred Tank. *Chem. Eng. Technol.*, 27, 225-231. DOI: 10.1002/ceat.200401992.

Fox R.O., 2003, *Computational model for turbulent reacting flows*, Cambridge University Press, Cambridge.

Jaworski Z., 2005. *Computational fluid dynamics in chemical and process engineering* (in Polish), Akademicka Oficyna Wydawnicza EXIT, Warszawa.

Lee K. C., Yianneskis M., 1998. Turbulence properties of the impeller stream of a Rushton turbine. *AIChE J.*, 44, 13-24. DOI: 10.1002/aic.690440104.

Mortensen M., Orciuch W., Bouaifi M., Andersson B., 2004. Mixing of a jet in a pipe. *Chem. Eng. Res. Des.*, 82, 357-363. DOI:10.1205/026387604322870462.

Wu H., Patterson G. K., 1989. Laser-Doppler measurements of turbulent-flow parameters in a stirred mixer. *Chem. Eng. Sci.*, 44, 2207-2221. DOI:10.1016/0009-2509(89)85155-3.